In Vivo Assessment of Glucose Metabolism in Hepatocellular Carcinoma with FDG-PET

Tatsuo Torizuka, Nagara Tamaki, Tetsuro Inokuma, Yasuhiro Magata, Satoshi Sasayama, Yoshiharu Yonekura, Akira Tanaka, Yoshio Yamaoka, Kazutaka Yamamoto and Junji Konishi

Department of Nuclear Medicine and Second Department of Surgery, Kyoto University Faculty of Medicine, Kyoto; and Department of Radiology, Fukui Medical School, Fukui, Japan

The present study was designed to assess glucose metabolism in hepatocellular carcinoma (HCC) with PET and [^{18}F]fluorodeoxyglucose (FDG) and to compare the results with the measured in vitro enzymatic activity of glucose metabolism and the histologic grading of HCC. **Methods:** Dynamic FDG-PET scans were obtained in 17 preoperative patients with HCC. From the serial tissue and arterial radioactivities obtained by dynamic PET, FDG kinetic rate constants (K1 to k4) were obtained. The standardized uptake value (SUV) was also determined from the images acquired 48 to 60 min after FDG administration. These PET results were compared with hexokinase and glucose-6-phosphatase (G6Pase) activities and histologic grading of HCC in surgically resected tumor materials. According to histologic grading, the tumors were divided into low-grade and high-grade HCCs. **Results:** The k3 and SUV of high-grade HCCs were significantly higher than those of low-grade HCCs ($p < 0.005$, each). In addition, high correlations were observed between the hexokinase activities and these two parameters ($r = 0.715$ 0.768, respectively). In some HCCs, relatively high G6Pase activities and k4 values modified tumor FDG uptake. **Conclusion:** FDG PET is a valuable method for assessing glucose metabolism and histologic grading of HCC.

Key Words: hepatocellular carcinoma; fluorine-18-fluorodeoxyglucose; positron emission tomography; glucose metabolism

J Nucl Med 1995; 36:1811–1817

It is well known that glycolysis is enhanced in rapidly growing tumors (*1*). This increase in glucose metabolism can be quantitatively assessed by PET with [^{18}F]fluorodeoxyglucose (FDG). DiChiro et al. (*2–4*) measured glucose metabolism of brain tumors with FDG-PET and found good correlation between glycolytic rate and tumor grade. Wahl et al. (*5*) assessed the efficacy of breast cancer treatment using sequential quantitative FDG-PET scans. Recent investigators quantitatively evaluated glucose utilization in liver tumors with dynamic FDG-PET and showed its usefulness for assessing characterization of tumor and therapeutic effect (*6,7*).

The liver is known to have increased activity of glucose-6-phosphatase (G6Pase) (*8*). Experimental studies demonstrate that glycogenesis decreases and glycolysis increases during carcinogenesis in the liver (*9,10*). Therefore, it might be important to determine whether glucose metabolism assessed by FDG-PET reflects the degree of differentiation of hepatocellular carcinoma (HCC). In the present study, glucose metabolism of HCC was quantitatively evaluated by FDG-PET, and the results were compared with in vitro enzymatic activity of glucose metabolism and histologic grading of HCC.

MATERIALS AND METHODS

Patients

Seventeen preoperative patients with HCC (15 men, 2 women) were studied. These patients ranged in age from 36 to 69 yr (mean 56 yr). Three of them had been untreated, and the other 14 patients had received interventional therapy more than 10 days before the PET study (mean interval 25 days). These 14 patients had received transcatheter arterial infusion of 3–5 ml iodized oil mixed with anticancer drugs. All tumors were greater than 3 cm in diameter on CT images. Surgery (hepatectomy or tumor enucleation) was performed after PET study (mean interval 13 days). Each subject gave written informed consent, and the study was approved by the Kyoto University Human Studies Committee.

Preparation of FDG

FDG was prepared as described previously (*11,12*). Briefly, after the production of [^{18}F]FDG was synthesized by the acetyl hydrofluorite method.

Study Protocol

The PET study was performed with a whole-body PET camera which had eight rings that provided 15 tomographic slices at 7-mm intervals with an intrinsic resolution of 4.6 mm FWHM. The spatial resolution of the reconstructed image was 12 mm FWHM and the axial resolution was 6 mm FWHM.

The patients fasted for at least 5 hr before the FDG injection. A transmission scan was obtained for 20 min with a rotating ^{68}Ge/^{68}Ga standard plate source to measure the attenuation factor. Without a change in the patient's position, a dynamic scan was acquired after intravenous administration of 150–250 MBq FDG. The dynamic sequence consisted of eight 30-sec scans and fourteen 4-min scans for a total scan time of 60 min. The reconstruction was performed with Shepp and Logan filter convoluted with

Received Sept. 13, 1994; revision accepted Jan. 16, 1995.

For correspondence or reprints contact: Tatsuo Torizuka, MD, Department of Nuclear Medicine, Kyoto University Faculty of Medicine, 54 Kawahara-cho, Shogoin, Sakyo-ku, Kyoto, 606 Japan.

gaussian function (sigma = 1.5). No accurate correction was made for tissue-blood volume. The serum glucose levels were measured just before tracer administration.

Data Analysis

PET images were compared with the corresponding CT images, which permitted accurate identification of the tumor by anatomic landmarks (for example, the upper pole of the kidney, the lower part of the heart and the shape of the gallbladder bed). For quantitative evaluation, a square region of interest (ROI) (12 × 12 mm) was placed over the area of maximal FDG uptake in the tumor. Areas of decreased or absent FDG uptake in the tumor, when present, were excluded from the ROI. A small square ROI (4 × 4 mm) was placed over the abdominal aorta to obtain an arterial input function.

In our previous FDG-PET study with arterial blood sampling (*13*), the ratio between the whole blood value and the plasma value (W/P ratio) was calculated for seven human subjects. The W/P ratio (0.91 ± 0.05) was constant in these subjects and did not change during the 60-min PET examination. Therefore, we used the mean value, 0.91, to correct the ROI measurement of abdominal aortic activity to the plasma value. To correct for partial volume effects associated with object's size, the diameter of the abdominal aorta measured by x-ray CT and the recovery coefficient obtained experimentally from phantom studies were used (*14*). The range of diameter of the abdominal aorta was 15 to 20 mm. For example, the recovery coefficient was 0.9 in abdominal aortas that were 15 mm in diameter. The true abdominal aortic activity was calculated as the observed tracer concentration divided by the recovery coefficient.

The analysis of the three-compartment model for FDG was made by the metabolic model of Phelps et al. (*15*). The rate constants that describe the transport between the compartments included K1 (in milliliters per minute per gram) and k2 (in reciprocal minutes) for forward and reverse FDG transport, k3 (in reciprocal minutes) and k4 (in reciprocal minutes) for phosphorylation of FDG and dephosphorylation of FDG-6-phosphate. With the arterial input function and successive values of tumor activity, the rate constants K1 to k4 were calculated with a Macintosh program and factorized quasi-Newton method.

From the images acquired 48 to 60 min after FDG administration, the standardized uptake value (SUV) was calculated in the ROI placed over the tumor. The SUV is the tissue activity (in millicuries per gram) divided by the injected dose (in millicuries) per body weight (in grams) (*16*).

Enzyme Activity Assays

In the resected tumor materials, the activities of key glucose-metabolizing enzymes, hexokinase and G6Pase, were measured in accordance with the methods of Vinuela et al. (*17*) and Koide et al. (*18*). After surgical resection, the material was obtained from the tumor slice corresponding to the ROI on the PET image.

Histologic Examination

Histologic examination was performed to assess the histologic grade of HCC. The material was obtained from the same tumor slice as that for the enzyme activity assay. Microscopic examination was performed with routine hematoxylin-eosin staining. According to histologic grade, the tumors were divided into low-grade HCCs (grade I, well-differentiated type; grade II, moderately differentiated type) and high-grade HCCs (grade III, poorly differentiated type; grade IV, undifferentiated type) (*19*).

Statistical Analysis

Comparisons of differences in the rate constants and enzymatic activity were performed with the Mann-Whitney test, and probability values less than 0.05 were considered to indicate statistical significance.

RESULTS

All the tumors showed greater increases in FDG uptake than the liver tissues on the late PET images. Figure 1 shows that FDG uptake of a high-grade HCC (undifferentiated type) increased with the time after tracer injection. By contrast, in Figure 2, FDG uptake of a low-grade HCC (moderately differentiated type) gradually decreased with the time postinjection but remained higher than the liver FDG uptake.

Histologic findings from the resected materials showed that viable HCC tissues were diffusely found, and necrotic or inflammatory tissues were scarcely seen. There were eight low-grade HCCs and nine high-grade HCCs (Table 1). In enzymatic studies, the hexokinase activities of the high-grade HCCs (0.74 ± 0.26 mU/mg) were significantly higher than those of the low-grade HCCs (0.36 ± 0.15 mU/mg, $p < 0.01$). The G6Pase activities of the high-grade HCCs (1.39 ± 1.26 mU/mg) tended to be lower than those of the low-grade HCCs (2.24 ± 1.09 mU/mg), although the difference was not significant. The G6Pase/HK ratios were significantly lower in the high-grade HCCs (2.10 ± 2.02) than in the low-grade HCCs (7.69 ± 4.63, $p < 0.01$). The time intervals between the therapy, PET scan and operation were not significantly different between these two groups.

Quantitative assessment of tumor FDG uptake and the histologic grade of HCC are summarized in Table 2. The k3 and SUV in the high-grade HCCs were significantly higher than those in the low-grade HCCs (0.057 ± 0.052 compared with 0.012 ± 0.004 and 6.89 ± 3.39 compared with 3.21 ± 0.58, respectively; $p < 0.005$, each). Although there was no significant difference in k4 values between the low- and high-grade HCCs (0.010 ± 0.005 compared with 0.012 ± 0.012), the k4/k3 ratios in the high-grade HCCs (0.287 ± 0.331) were significantly lower than those in the low-grade HCCs (0.853 ± 0.559, $p < 0.005$). Two high-grade HCCs with low k3 values (<0.016) showed low k4 values (<0.004), whereas three low-grade HCCs with high k3 values (>0.015) showed high k4 values (>0.009). The K1 and k2 values were significantly greater in the low-grade HCCs than in the high-grade HCCs (0.470 ± 0.205 versus 0.283 ± 0.066 and 0.533 ± 0.169 compared with 0.371 ± 0.174, respectively; $p < 0.05$, each).

When the HK activities were compared with the k3 and SUV, high correlations were observed ($r = 0.715$ and 0.768, respectively; Figs. 3 and 4). Although there was no significant relationship between the G6Pase activities and k4 values ($r = 0.173$), the G6Pase/hexokinase ratios were closely correlated with the k4/k3 ratios ($r = 0.653$, Fig. 5).

The mean plasma glucose concentration was 103 mg/dl. Two patients had high glucose concentrations (201 and 149

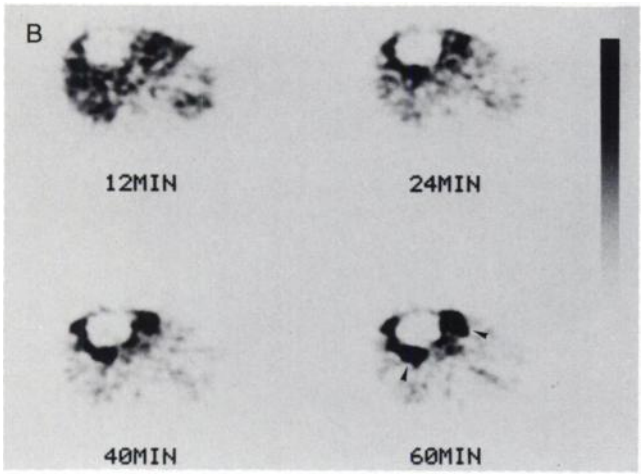

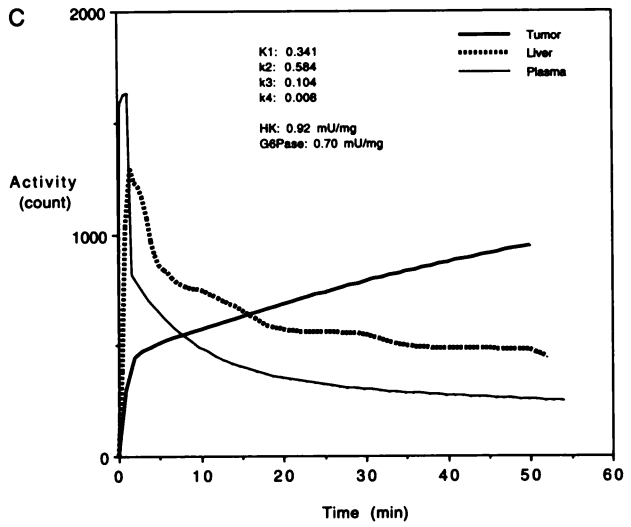

FIGURE 1. (A) CT image of huge HCC, heterogeneous region (arrowheads) shows a little Lipiodol deposit around the low-density area. (B) Dynamic PET images. (C) Time-activity curves of FDG uptake. Tumor FDG uptake (arrowheads), which corresponds to heterogeneous region on CT, increases with time after tracer injection, whereas FDG uptake of the liver and plasma decrease with time postinjection. Tumor shows high k3 value and HK activity. FDG defect, which corresponds to low-density area on CT, was proved to be necrosis after routine histologic examination.

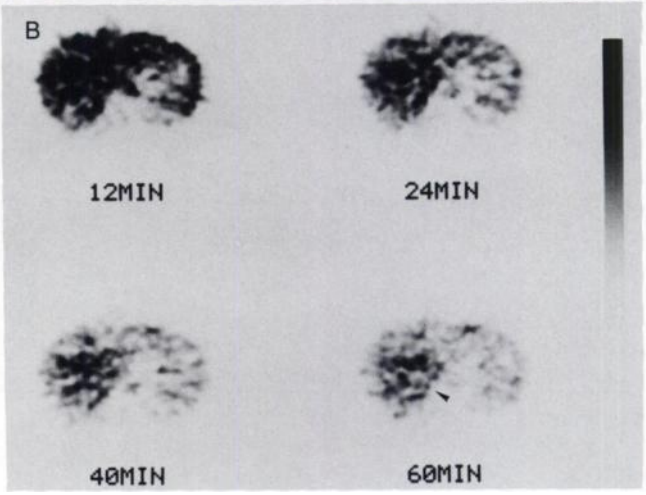

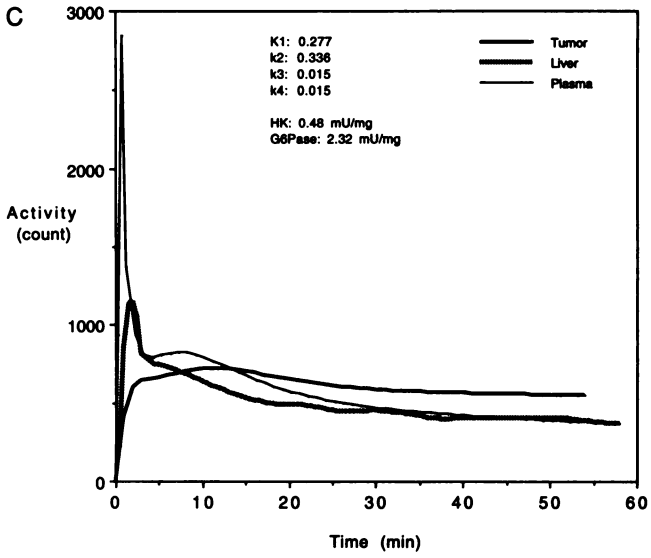

FIGURE 2. (A) CT image shows huge HCC with little Lipiodol deposit in right lobe of liver. (B) Dynamic PET images. (C) Time-activity curves of FDG uptake. FDG uptake of liver and plasma decrease with time postinjection. Tumor FDG uptake (arrow-head) also gradually decreases but remains higher than liver FDG uptake. Compared with tumor shown in Figure 1, k3 value and HK activity are lower, whereas k4 value and G6Pase activity are higher.

TABLE 1
Histologic Grade of Hepatocellular Carcinoma and Enzymatic Activity

Patient no.	Histologic grade*	Tumor size (cm)	Enzymatic activity HK (mU/mg)	Enzymatic activity G6Pase (mU/mg)	Enzymatic activity G6Pase/HK	Serum glucose level (mg/dl)
1	Grade I	3	0.28	3.48	12.43	105
2	Grade I	4	0.18	2.22	12.33	90
3	Grade II	3	0.27	1.18	4.37	95
4	Grade II	3	0.62	1.17	1.89	149
5	Grade II	3	0.53	1.11	2.09	88
6	Grade II	10	0.31	4.32	13.94	86
7	Grade II	18	0.48	2.32	4.83	83
8	Grade II	4	0.22	2.13	9.68	97
Mean ± s.d.		6 ± 5.05	0.36 ± 0.15	2.24 ± 1.09	7.69 ± 4.63	99 ± 20
9	Grade III†	3	0.41	0.33	0.8	92
10	Grade III	5	0.6	0.36	0.6	96
11	Grade III	4	0.38	2.23	5.87	95
12	Grade III	3	0.79	4.54	5.75	133
13	Grade III	16	0.88	1.56	1.77	84
14	Grade III	15	1.19	1.44	1.21	102
15	Grade IH	18	0.5	0.81	1.62	60
16	Grade IV	18	0.97	0.53	0.55	201
17	Grade IV	15	0.92	0.7	0.76	98
Mean ± s.d.		10.78 ± 6.39	0.74 ± 0.26	1.39 ± 1.26	2.1 ± 2.02	107 ± 38
p value		ns	<0.01	ns	<0.01	ns

*Grades I and II are low grade.
†Grades III and IV are high grade.
HK = hexose kinase; G6Pase = glucose-6-phosphatase; ns = not significant.

mg/dl) because of diabetes mellitus, but the K1 to k4 and SUV in these patients were within the mean values ± 2 s.d. of the remaining patients' data.

DISCUSSION

This study demonstrated that quantitative assessment of glucose metabolism by FDG-PET highly reflected the enzymatic activity of glucose metabolism and the histologic grading of HCC.

Glucose Metabolism of HCC

Early observations by Warburg et al. (*1*) and others (*20,21*) demonstrated that aerobic glycolysis was increased in malignant tumors. FDG, a glucose analog, is transported into the tumor cells and turned into FDG-6-phosphate by glycolytic enzymes. It is not, however, further metabolized and is trapped in the tumor tissue. On the other hand, FDG accumulation is decreased in the nontumor liver tissue because the liver has a high G6Pase concentration (*8*). Weber and Cantero (*9*) and Weber and Morris (*10*) demonstrated in their experimental studies that the glycogene-

TABLE 2
Fluorodeoxyglucose Uptake Measures for Low- and High-Grade Hepatocellular Carcinomas

Parameter	Low grade	High grade	p value
K1	0.47 ± 0.205	0.283 ± 0.066	<0.05
k2	0.533 ± 0.169	0.371 ± 0.174	<0.05
k3	0.012 ± 0.004	0.057 ± 0.052	<0.005
k4	0.01 ± 0.005	0.012 ± 0.012	ns
k4/k3	0.853 ± 0.559	0.287 ± 0.331	<0.005
SUV	3.21 ± 0.58	6.89 ± 3.39	<0.005

ns = not significant; SUV = standardized uptake value.

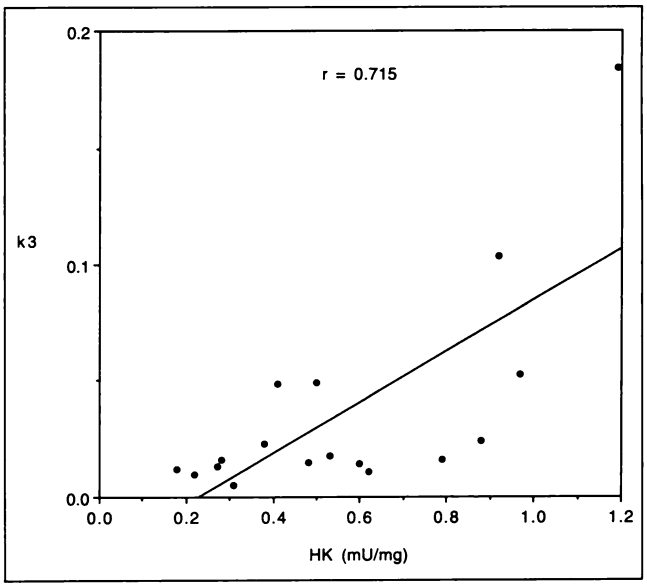

FIGURE 3. Correlation of rate constant k3 and HK activity.

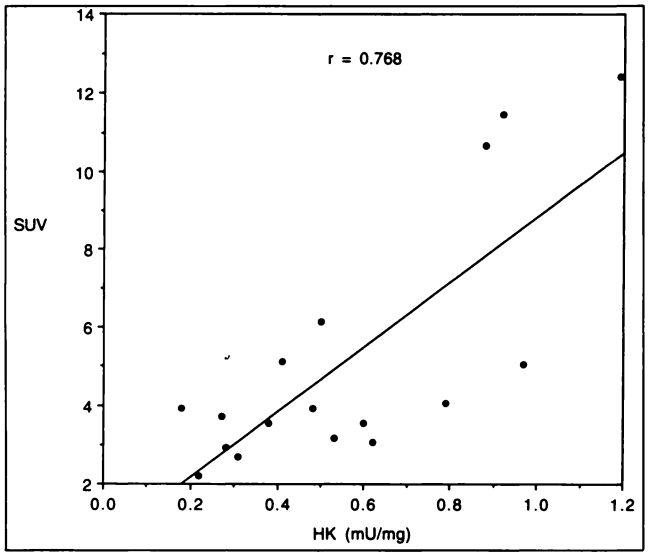

FIGURE 4. Correlation of SUV and HK activity.

sis of liver decreased during carcinogenesis and was almost completely absent in HCC. These differences may result in increased accumulations of FDG in HCC (*6,22*) and metastatic liver tumors (*23,24*) on PET images. We previously reported that FDG-PET is valuable to monitor HCC after interventional therapy (*25*). In a dynamic PET study, Okazumi et al. (*6*) indicated that, malignant liver tumors had significantly higher values of the rate constant k3 than did benign liver tumors, but they did not show the relationship between the PET results and histologic grading of HCC.

Table 2 shows that the k3 and SUV were significantly higher in the high-grade HCCs. In addition, HK activities in the high-grade HCCs were significantly greater than those in the low-grade HCCs (Table 1), and high correlations were observed between the hexokinase activities and these two parameters (Figs. 3 and 4). These results agree

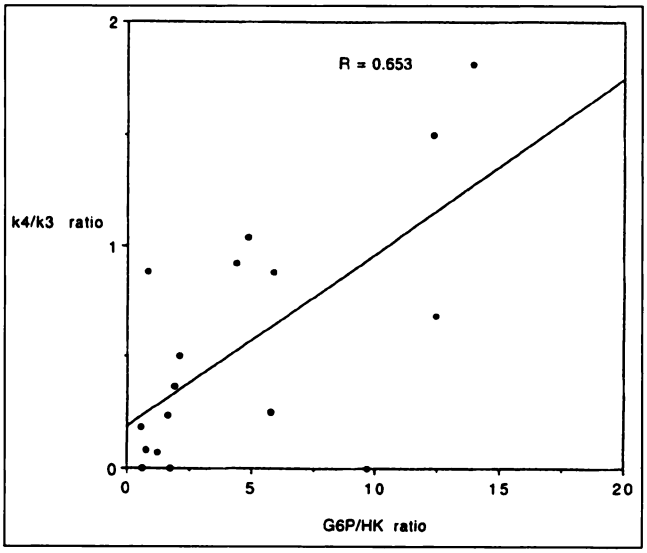

FIGURE 5. Correlation of k4/k3 ratio and G6Pase/HK ratio.

with the early experimental observations that glycolysis is increased in rapidly growing hepatomas (*26,27*). The FDG rate constants in tumors assessed by PET may estimate enzymatic activities (*6*) and, therefore, reflect the histologic grading of HCC well.

It was demonstrated that k4 may be useful to distinguish HCC from other liver tumors with k4 values of nearly zero (*6*). In Table 1, the G6Pase activities of low-grade HCCs tended to be higher than those of high-grade HCCs, which suggests that low-grade HCCs may retain the properties of normal liver tissue. Although k4 did not correlate with the G6Pase activities, the k4/k3 ratios in the high-grade HCCs were significantly lower than those in the low-grade HCCs (Table 2). In addition, two of the high-grade HCCs showed low k3 and k4 values; three of the low-grade HCCs showed high k3 and k4 values. These results suggest that FDG uptake in some HCCs may be modified by k4 and k3. Therefore, to assess the glycogenesis and the histologic grading of HCC, it may be necessary to calculate both k3 and k4 by dynamic FDG PET.

Preoperative treatments for HCC are often performed to decrease the tumor's activity, which thereby makes hepatic resection both easier and safer (*28,29*). In this study, 14 of 17 tumors had received the interventional therapy more than 10 days before the PET study. The histologic findings obtained from the resected materials showed that viable HCC tissues were diffusely present, and necrotic or inflammatory tissues were seldom observed. These data suggest that the therapy was not as effective on the areas of maximal FDG uptake in the tumors.

Technical Considerations

In the present study, we used a three-compartment metabolic model proposed for the normal brain. Although the rate constants k3 and k4 reflected glucose metabolism in HCC well, high variability of the K1 to k4 values was observed. These findings were in accord with the previous observations by Okazumi et al. (*6*). Because glycolytic enzyme activity in tumor tissue is heterogeneous (*30*) and glucose metabolic rates vary largely (*31,32*), the results of tumor FDG kinetic studies may be influenced by tissue heterogeneity. Only a few studies of tissue heterogeneity effects with cerebral deoxyglucose uptake, however, have been reported (*33,34*).

Recent studies have used SUV, which relates tissue radioactivity to injected dose and body weight, to classify the tumor and to monitor the response to treatment (*35,36*). This index has the advantage of technical simplicity, without any need for arterial blood sampling or complicated models. The SUV, however, is dependent on body weight (*37*) and the time difference between FDG injection and image acquisition (*38*). SUV should be measured after tumor FDG uptake has reached a plateau, when the concentration of FDG in the tumor is independent of the details of FDG transport. Because SUVs of some HCCs are considered to be modified by k4 and k3, further study may

be necessary to determine the most adequate time of SUV measurement in HCC.

The liver has two systems of blood supply (the hepatic artery and the portal vein), and thus it is better to use data from these two systems as the input function. It is clinically difficult, however, to measure them separately in patients during PET scanning. We used data from the arterial input function because HCCs are supplied largely by the hepatic artery (*39*). The FDG rate constants in liver tissue were not calculated because of the two systems of blood supply.

The limited resolution of the PET scanner and patient respiratory movement may provide inherent limitations for the analysis of small tumors. Therefore, tumors less than 3 cm in diameter were excluded from this study. In our results, tumors with K1 > 0.5 or k2 > 0.6 were all 3–4 cm in diameter, probably because the K1 and k2 values in these small tumors might be substantially influenced by the blood flow of the surrounding liver tissue. Tables 1 and 2 show that the low-grade HCCs, including six smaller tumors, had significantly higher values of K1 and k2 than the high-grade HCCs, including five larger tumors more than 15 cm in diameter.

CONCLUSION

In this comparative study, FDG-PET results were related to the in vitro enzymatic activity of glucose metabolism and reflected the histologic grading of HCC well. Although SUV is a simple index to assess tumor metabolism, the rate constants k3 and k4 may be also valuable indices, especially in HCCs with high k4 values.

ACKNOWLEDGMENTS

The authors thank the Cyclotron staff for their technical assistance. This work was supported in part by a grant-in-aid from the Ministry of Education, Science and Culture, Tokyo, Japan.

REFERENCES

1. Warburg O, Wind F, Negelein E. On the metabolism of tumors in the body. In: Warburg O, ed. *The metabolism of tumors.* London: Constable; 1930: 254–270.
2. DiChiro G, DeLaPaz RL, Brooks RA, et al. Glucose utilization of cerebral gliomas measured by [^{18}F] fluorodeoxyglucose and positron emission tomography. *Neurology* 1982;32:1323–1329.
3. DiChiro G, Brooks RA, Patronas NJ, et al. Issues in the in vivo measurement of glucose metabolism of human central nervous system tumors. *Ann Neurol* 1984;15(suppl):s138–s146.
4. DiChiro G. Positron emission tomography using [^{18}F] fluorodeoxyglucose in brain tumors: a powerful diagnostic and prognostic tool. *Invest Radiol* 1986;22:360–371.
5. Wahl RL, Zasadny K, Helvie M, et al. Metabolic monitoring of breast cancer chemohormonotherapy using positron emission tomography: initial evaluation. *J Clin Oncol* 1993;11:2101–2111.
6. Okazumi S, Isono K, Enomoto K, et al. Evaluation of liver tumors using fluorine-18-fluorodeoxy-glucose PET: characterization of tumor and assessment of effect of treatment. *J Nucl Med* 1992;33:333–339.
7. Messa C, Choi Y, Hoh CK, et al. Quantification of glucose utilization in liver metastases: parametric imaging of FDG uptake with PET. *J Comput Assist Tomogr* 1992;16:684–689.
8. Gallagher BM, Fowler JS, Gutterson NI, et al. Metabolic trapping as a principle of radiopharmaceutical design: some factors responsible for the biodistribution of [^{18}F] 2-deoxy-2-fluoro-D-glucose. *J Nucl Med* 1978;19: 1154–1161.
9. Weber G, Cantero A. Glucose-6-phosphatase activity in normal, precancerous, and neoplastic tissues. *Cancer Res* 1955;15:105–108.
10. Weber G, Morris HP. Comparative biochemistry of hepatomas III. Carbohydrate enzymes in liver tumors of different growth rates. *Cancer Res* 1963;23:987–994.
11. Yonekura Y, Tamaki N, Kambara H, et al. Detection of metabolic alteration in ischemic myocardium by F-18 fluorodeoxyglucose uptake with positron emission tomography. *Am J Card Imaging* 1988;2:122–132.
12. Tamaki N, Yonekura Y, Yamashita K, et al. Relation of left ventricular perfusion and wall motion with metabolic activity in persistent defects on thallium-201 tomography in healed myocardium infarction. *Am J Cardiol* 1988;62:202–208.
13. Takahashi N, Tamaki N, Kawamoto M, et al. Noninvasive and simple method for the estimation of myocardial metabolic rate of glucose by PET and F-18 FDG. *Jpn J Nucl Med* 1994;31:985–990.
14. Hoffman EJ, Huang SC, Phelps ME. Quantitation in positron emission computed tomography: I. Effect of object size. *J Comput Assist Tomogr* 1979;3:299–308.
15. Phelps ME, Huang SC, Hoffman EJ, et al. Tomographic measurements of local cerebral glucose metabolic rate in humans with [F18]-2-fluoro-2-deoxy-D-glucose: validation of method. *Ann Neurol* 1979;6:371–388.
16. Kubota K, Matsuzawa T, Ito M, et al. Lung tumor imaging by positron emission tomography using C-11 L-Methionine. *J Nucl Med* 1985;26:37–42.
17. Vinuela E, Salas M, Sols A. Glucokinase and hexokinase in liver in relation to glycogen synthesis. *J Biol Chem* 1963;238:1175.
18. Koide H, Oda T. Pathological occurrence of glucose-6-phosphatase in serum in liver diseases. *Clin Chim Acta* 1959;4:554–561.
19. Edmondson HA. *Tumors of the liver and intrahepatic bile duct.* Washington: Armed Forces Institute of Pathology; 1958:32–104.
20. Sharma RM, Sharma C, Donnelly AJ, Morris HP, Weinhouse S. Glucose-ATP phosphotransferases during hepatocarcinogenesis. *Cancer Res* 1965; 25:193–199.
21. Criss WE. A review of isozymes in cancer. *Cancer Res* 1971;31:1523–1542.
22. Nagata Y, Yamamoto K, Hiraoka M, et al. Monitoring liver therapy with [F18]FDG positron emission tomography. *J Comput Assist Tomogr* 1990; 14:370–374.
23. Yonekura Y, Benua RS, Brill AB, et al. Increased accumulation of 2-deoxy-2-[F18]fluoro-D-glucose in liver metastasis from colon carcinoma. *J Nucl Med* 1982;23:1133–1137.
24. Strauss LG, Conti PS. The applications of PET in clinical oncology. *J Nucl Med* 1991;32:623–648.
25. Torizuka T, Tamaki N, Inokuma T, et al. Value of fluorine-18-FDG-PET to monitor hepatocellular carcinoma after interventional therapy. *J Nucl Med* 1994;35:1965–1969.
26. Shonk CE, Morris HP, Boxer CE. Patterns of glycolytic enzymes in rat liver and hepatoma. *Cancer Res* 1965;25:671–676.
27. Burk D, Woods M, Hunter J. On the significance of glucolysis for cancer growth, with special reference to Morris rat hepatomas. *J Natl Cancer Inst* 1967;38:839–863.
28. Sasaki Y, Imaoka S, Kasugai H, et al. A new approach to chemoembolization therapy for hepatoma using ethiodized oil, cisplatin and gelatin sponge. *Cancer* 1987;60:1194–1203.
29. Choi BI, Kim HC, Han JK, et al. Therapeutic effect of transcatheter oily chemoembolization therapy for encapsulated nodular hepatocellular carcinoma: CT and pathologic findings. *Radiology* 1992;182:709–713.
30. Fidler I. The biology of human cancer metastasis. *Acta Oncol* 1991;6:669–675.
31. Herholz K, Ziffling P, Staffen W, et al. Uncoupling of hexose transport and phosphorylation in human gliomas demonstrated by PET. *Eur J Cancer* 1988;7:1139–1150.
32. Lammertsma AA, Brooks DJ, Frackowiak RSJ, et al. Measurement of glucose utilization with [^{18}F]2-fluoro-2-deoxy-D-glucose: a comparison of different analytical methods. *J Cereb Blood Flow Metab* 1987;7:161–172.
33. Herholz K, Patlak CS. The influence of tissue heterogeneity on results of fitting nonlinear model equations to regional tracer uptake curves: with an application to compartmental models used in positron emission tomography. *J Cereb Blood Flow Metab* 1987;7:214–229.
34. Schmidt K, Mies G, Sokoloff L. Model of kinetic behavior of deoxyglucose in heterogeneous tissues in brain: a reinterpretation of the significance of parameters fitted to homogeneous tissue models. *J Cereb Blood Flow Metab* 1991;11:10–24.
35. Adler LP, Blair HF, Makley JT, et al. Noninvasive grading of musculoskeletal tumors using PET. *J Nucl Med* 1991;32:1508–1512.
36. Haberkorn U, Strauss LG, Dimitrakopoulou A, et al. PET studies of fluo-

rodeoxyglucose metabolism in patients with recurrent colorectal tumors receiving radiotherapy. *J Nucl Med* 1991;32:1485–1490.
37. Zasadny KR, Wahl RL. Standardized uptake values of normal tissues at PET with 2-[fluorine-18]-fluoro-2-deoxy-D-glucose: variations with body weight and a method for correction. *Radiology* 1993;189:847–850.
38. Hamberg LM, Hunter GJ, Alpert NM, et al. The dose uptake ratio as an index of glucose metabolism: useful parameter or oversimplification? *J Nucl Med* 1994;35:1308–1312.
39. Breedis C, Young G. The blood supply of neoplasms in the liver. *Am J Pathol* 1954;30:969–985.

(continued from page 1739)

FIRST IMPRESSIONS:
EVALUATION OF RENAL OBSTRUCTION

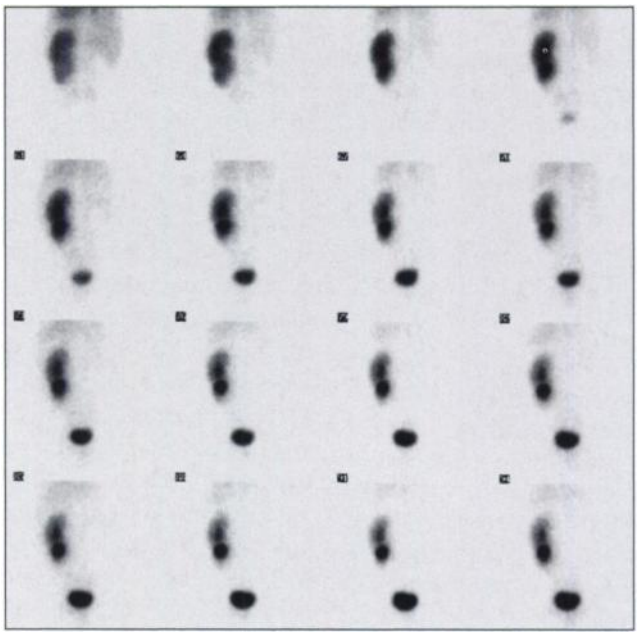

PURPOSE
A 5-yr-old boy was referred for evaluation of renal obstruction. Sequential posterior images (Fig. 1) depict an absence of tracer uptake in the right renal bed. The left kidney which appears to be elongated with irregular cortical outline actually represents two fused kidneys lying in the normal position of the left kidney (a crossed-fused ectopia). The upper kidney shows good uptake and excretion. The lower kidney shows slightly diminished initial uptake, possibly due to its more anterior position. Prolonged tracer retention is noted in the lower kidney collecting system but with no obstruction, as evidenced by prompt response to lasix (not shown).

TRACER
Technetium-99m-DTPA, 5.9 mCi

ROUTE OF ADMINISTRATION
Intravenous

TIME AFTER INJECTION
Two minutes per frame for 32 minutes

INSTRUMENTATION
Vision 1024 RZ, Summit Nuclear

CONTRIBUTORS
Mordechai Lorberboym and Chun K. Kim, The Mount Sinai Medical Center, New York, NY